Rare semileptonic decays of B and B_c mesons in the relativistic quark model

D. Ebert[1], R. N. Faustov[1,2] and V. O. Galkin[1,2]

[1] *Institut für Physik, Humboldt–Universität zu Berlin,*
Newtonstr. 15, D-12489 Berlin, Germany
[2] *Dorodnicyn Computing Centre, Russian Academy of Sciences,*
Vavilov Str. 40, 119991 Moscow, Russia

Rare semileptonic decays of B and B_c mesons are investigated in the framework of the QCD-motivated relativistic quark model based on the quasipotential approach. Form factors parametrizing the matrix elements of the weak transitions between corresponding meson states are calculated with the complete account of the relativistic effects including contributions of intermediate negative energy states and relativistic transformations of the meson wave functions. The momentum transfer dependence of the form factors is reliably determined in the whole accessible kinematical range. On this basis the total and differential branching fractions of the $B \to K^{(*)} l^+ l^- (\nu\bar{\nu})$ and $B_c \to D_s^{(*)} l^+ l^- (\nu\bar{\nu})$, $B_c \to D^{(*)} l^+ l^- (\nu\bar{\nu})$ decays as well as the longitudinal polarization fractions F_L of the final vector meson and the muon forward-backward asymmetries A_{FB} are calculated. Good agreement of the obtained results with the recent detailed experimental data on the $B \to K^{(*)} \mu^+ \mu^-$ decays from Belle and CDF is found. Predictions for the rare semileptonic decays of the B_c mesons are given.

PACS numbers: 13.20.He, 12.39.Ki

I. INTRODUCTION

The investigation of the rare weak B and B_c meson decays represents a very interesting and important problem. Such decays are governed by the flavour-changing neutral currents, which are forbidden at tree level in the standard model (SM) and first appear at one-loop. Therefore, such decays are very sensitive to the contributions of new intermediate particles and interactions, predicted in numerous extensions of the SM (see e.g. [1, 2] and references therein). Notwithstanding the fact that such decays have very small branching ratios, comparison of existing theoretical and experimental results for the rare semileptonic and radiative $B \to K^{(*)}$ decays already provides one of the most rigid constraints on different new physics scenarios [3].

The theoretical analysis of the rare weak B decays is based on the electroweak effective Hamiltonian, which is obtained by integrating out the heavy degrees of freedom (electroweak bosons and top quark) [3]. The QCD corrections to these processes due to hard gluon exchanges turn out to be important and require to resum large logarithms, which is done with the help of renormalization group methods. The operator product expansion allows to separate the short-distance part in the B meson decay amplitudes, which is described by the Wilson coefficients and can be calculated perturbatively, from the long-distance

part contained in the operator matrix elements between initial and final meson states. For the investigation of the exclusive decay rates one needs to apply nonperturbative methods to calculate these hadronic matrix elements which are usually parametrized in terms of covariant form factors. Clearly, such calculation is model dependent. In order to reduce model dependence, methods, based on the heavy quark and large energy expansions, have been developed. They employ the new symmetries which arise in heavy quark and large energy limits and permit to significantly reduce the number of independent form factors [4]. Such methods allow a perturbative calculation of QCD corrections to the factorization approximation and thus are now popular in the literature [5]. However, the important Λ_{QCD}/m_b corrections cannot be systematically taken into account in such an approach.

Rare $B \to K^{(*)}$ transitions are the most studied ones both theoretically and experimentally [3]. Recently, detailed experimental data on differential branching fractions, angular distributions and asymmetries in the rare $B \to K^{(*)}\mu^+\mu^-$ decays became available both from B factories and Tevatron [6–9]. The measured values are at present consistent with the predictions of the SM within experimental and theoretical uncertainties. Significantly better statistics on the rare B decays is expected form LHC experiments (especially from LHCb) which will allow precision tests of the SM and can probably reveal signals of new physics [10]. It is expected that the B_c mesons will be copiously produced at LHC, making possible the experimental study of their weak rare decays. Such decays received significantly less attention in the literature. The $B_c \to D_s^{(*)}l^+l^-$ and $B_c \to D^{(*)}l^+l^-$ were previously investigated using the relativistic constituent quark model [11], light-front quark model [12, 13] and three-point QCD sum rules [14].

In this paper we study the rare weak B and B_c decays in the framework of the QCD-motivated relativistic quark model. Our model was previously successfully applied for the investigation of various electroweak properties of heavy and light hadrons. Semileptonic decay rates of the B [15] and B_c [16, 17] mesons as well as rare radiative decays of the B [18] were calculated in agreement with available experimental data. For this purpose, effective methods of the calculation of electroweak matrix elements between meson states with a consistent account of relativistic effects were developed. They allow to reliably determine the form factor dependence on the momentum transfer in the whole accessible kinematical range. The form factors are expressed as overlap integrals of the meson wave functions, which were obtained in the corresponding calculations of the mass spectra [19, 20]. It is important to note that we specially checked [21, 22] the fulfillment of the model-independent symmetry relations among form factors arising in the heavy quark and large energy limits. Here we apply these methods to the calculation of the form factors of the rare $B \to K^{(*)}$ and $B_c \to D_s^{(*)}(D^{(*)})$ transitions and on this basis determine branching fractions and differential distributions of these decays.

The paper is organized as follows. The relevant effective weak Hamiltonian for the rare B and B_c decays is briefly discussed in Sec. II. In Sec. III we give an outline of our relativistic quark model. Then in Sec. IV we discuss the relativistic calculation of the hadronic matrix element of the weak current between meson states in the quasipotential approach. Special attention is devoted to the contributions of negative energy states and the relativistic transformation of the wave functions from the rest to the moving reference frame. Form factors of the rare semileptonic $B \to K^{(*)}$ and $B_c \to D_s^{(*)}(D^{(*)})$ decays are calculated in Sec. V. These form factors are used in Sec. VI for the calculation of the total and differential rare decay branching fractions. First we give the necessary formulas and then present our numerical results. These are then confronted with available experimental data and predictions

3

of other approaches. Finally, Sec. VII contains our conclusions. Expressions for the tensor form factors of the rare B and B_c meson decays in terms of the overlap integrals of meson wave functions are given in the Appendix.

II. EFFECTIVE HAMILTONIAN FOR THE RARE B AND B_c MESON DECAYS

The usual approach to the description of rare B decays is based on the low-energy effective Hamiltonian, obtained by integrating out the heavy degrees of freedom (the top quark and W bosons) of the SM. The operator product expansion separates the short-distance contributions, which are contained in the Wilson coefficients and can be calculated perturbatively, from the long-distance contributions contained in the matrix elements of the local operators. The calculation of such matrix elements requires the application of nonperturbative methods.

The effective Hamiltonians for $b \to f l^+ l^-$ and $b \to f \nu \bar{\nu}$ transitions ($f = s$ or d), renormalized at a scale $\mu \approx m_b$, are given by [23]

$$
\begin{aligned}
\mathcal{H}_{\text{eff}}^{l^+l^-} &= -\frac{4G_F}{\sqrt{2}} V_{tf}^* V_{tb} \sum_{i=1}^{10} C_i \mathcal{O}_i, \\
\mathcal{H}_{\text{eff}}^{\nu\bar{\nu}} &= -\frac{4G_F}{\sqrt{2}} V_{tf}^* V_{tb} C_L^\nu \mathcal{O}_L^\nu,
\end{aligned}
\tag{1}
$$

where G_F is the Fermi constant, V_{tj} are Cabibbo-Kobayashi-Maskawa matrix elements, C_i are the Wilson coefficients and $\mathcal{O}_i$ are the standard model operator basis which can be found e.g. in [24]. The most important operators for the $b \to f l^+ l^-$ transitions are the following

$$
\begin{aligned}
\mathcal{O}_7 &= \frac{e}{32\pi^2} m_b (\bar{f} \sigma_{\mu\nu} (1+\gamma_5) b) F^{\mu\nu}, \\
\mathcal{O}_9 &= \frac{e^2}{32\pi^2} (\bar{f} \gamma_\mu (1-\gamma_5) b)(\bar{l} \gamma^\mu l), \\
\mathcal{O}_{10} &= \frac{e^2}{32\pi^2} (\bar{f} \gamma_\mu (1-\gamma_5) b)(\bar{l} \gamma^\mu \gamma_5 l),
\end{aligned}
\tag{2}
$$

with $F_{\mu\nu}$ being the electromagnetic field strength tensor, and for the $b \to f \nu \bar{\nu}$ transitions we have

$$
\mathcal{O}_L^\nu = \frac{e^2}{32\pi^2} (\bar{f} \gamma_\mu (1-\gamma_5) b)(\bar{\nu} \gamma^\mu (1-\gamma_5) \nu).
\tag{3}
$$

The resulting structure of the free quark decay amplitude has the form:

$$
\begin{aligned}
M(b \to f l^+ l^-) &= \frac{G_F}{\sqrt{2}} \frac{\alpha}{2\pi} V_{tf}^* V_{tb} \Big[C_9^{\text{eff}} (\bar{f} \gamma_\mu (1-\gamma_5) b)(\bar{l} \gamma^\mu l) + C_{10} (\bar{f} \gamma_\mu (1-\gamma_5) b)(\bar{l} \gamma^\mu \gamma_5 l) \\
&\quad - \frac{2m_b}{q^2} C_7^{\text{eff}} (\bar{f} \sigma_{\mu\nu} q^\nu (1+\gamma_5) b)(\bar{l} \gamma^\mu l) \Big], \\
M(b \to f \nu \bar{\nu}) &= \frac{G_F}{\sqrt{2}} \frac{\alpha}{2\pi} V_{tf}^* V_{tb} C_L^\nu (\bar{f} \gamma_\mu (1-\gamma_5) b)(\bar{\nu} \gamma^\mu (1-\gamma_5) \nu),
\end{aligned}
\tag{4}
$$

where α is the fine structure constant.

The effective Wilson coefficient C_7^{eff} is given [25] by $C_7^{\text{eff}} = C_7 - C_5/3 - C_6$, while C_9^{eff} accounts for both perturbative and certain long-distance contributions from the matrix elements of four-quark operators $\mathcal{O}_{1,...,6}$. The long-distance (nonperturbative) effects arise

from the $c\bar{c}$ resonance contributions from $J/\psi, \psi' \ldots$ and are usually assumed to have a phenomenological Breit-Wigner structure. Therefore C_9^{eff} reads as follows [11, 25, 26]

$$C_9^{\text{eff}} = C_9 + \mathcal{Y}_{\text{pert}}(q^2) + \mathcal{Y}_{\text{BW}}(q^2). \tag{5}$$

Here the perturbative part is given by

$$\begin{aligned}
\mathcal{Y}_{\text{pert}}(q^2) = \; & h\left(\frac{m_c}{m_b}, \frac{q^2}{m_b^2}\right)(3C_1 + C_2 + 3C_3 + C_4 + 3C_5 + C_6) \\
& -\frac{1}{2}h\left(1, \frac{q^2}{m_b^2}\right)(4C_3 + 4C_4 + 3C_5 + C_6) \\
& -\frac{1}{2}h\left(0, \frac{q^2}{m_b^2}\right)(C_3 + 3C_4) + \frac{2}{9}(3C_3 + C_4 + 3C_5 + C_6),
\end{aligned} \tag{6}$$

and the $c\bar{c}$ resonance part reads

$$\mathcal{Y}_{\text{BW}}(q^2) = \frac{3\pi}{\alpha^2} \sum_{V_i=J/\psi, \psi'} \frac{\Gamma(V_i \to l^+ l^-) M_{V_i}}{M_{V_i}^2 - q^2 - i M_{V_i} \Gamma_{V_i}}, \tag{7}$$

and q^2 is the four-momentum squared of the lepton pair, $m_{b,c}$ are the masses of the b and c quarks. The explicit form of the function $h(m_c/m_b, q^2/m^2)$ [27] and the values of Wilson coefficients $C_{1,\ldots,10}$ are given in Refs. [11, 25].

For the application of the above expressions to the description of the exclusive rare semileptonic decays of the B and B_c mesons it is necessary to calculate the matrix elements of the operators $\bar{f}\gamma_\mu(1-\gamma_5)b$ and $\bar{f}\sigma_{\mu\nu}q^\nu(1-\gamma_5)b$ between initial and final hadron states. Such calculation requires the application of nonperturbative approaches. In this paper we use the relativistic quark model based on the quasipotential approach for these investigations.

III.   RELATIVISTIC QUARK MODEL

In the quasipotential approach a meson is described as a bound quark-antiquark state with a wave function satisfying the quasipotential equation of the Schrödinger type

$$\left(\frac{b^2(M)}{2\mu_R} - \frac{\mathbf{p}^2}{2\mu_R}\right)\Psi_M(\mathbf{p}) = \int \frac{d^3q}{(2\pi)^3} V(\mathbf{p}, \mathbf{q}; M)\Psi_M(\mathbf{q}), \tag{8}$$

where the relativistic reduced mass is

$$\mu_R = \frac{E_1 E_2}{E_1 + E_2} = \frac{M^4 - (m_1^2 - m_2^2)^2}{4M^3}, \tag{9}$$

and E_1, E_2 are the center of mass energies on mass shell given by

$$E_1 = \frac{M^2 - m_2^2 + m_1^2}{2M}, \quad E_2 = \frac{M^2 - m_1^2 + m_2^2}{2M}. \tag{10}$$

Here $M = E_1 + E_2$ is the meson mass, $m_{1,2}$ are the quark masses, and $\mathbf{p}$ is their relative momentum. In the center of mass system the relative momentum squared on mass shell reads

$$b^2(M) = \frac{[M^2 - (m_1 + m_2)^2][M^2 - (m_1 - m_2)^2]}{4M^2}. \tag{11}$$

The kernel $V(\mathbf{p}, \mathbf{q}; M)$ in Eq. (8) is the quasipotential operator of the quark-antiquark interaction. It is constructed with the help of the off-mass-shell scattering amplitude, projected onto the positive energy states. Constructing the quasipotential of the quark-antiquark interaction, we have assumed that the effective interaction is the sum of the usual one-gluon exchange term with the mixture of long-range vector and scalar linear confining potentials, where the vector confining potential contains the Pauli interaction. The quasipotential is then defined by [19]

$$V(\mathbf{p}, \mathbf{q}; M) = \bar{u}_1(p)\bar{u}_2(-p)\mathcal{V}(\mathbf{p}, \mathbf{q}; M)u_1(q)u_2(-q), \tag{12}$$

with

$$\mathcal{V}(\mathbf{p}, \mathbf{q}; M) = \frac{4}{3}\alpha_s D_{\mu\nu}(\mathbf{k})\gamma_1^\mu\gamma_2^\nu + V_{\text{conf}}^V(\mathbf{k})\Gamma_1^\mu\Gamma_{2;\mu} + V_{\text{conf}}^S(\mathbf{k}),$$

where α_s is the QCD coupling constant, $D_{\mu\nu}$ is the gluon propagator in the Coulomb gauge

$$D^{00}(\mathbf{k}) = -\frac{4\pi}{\mathbf{k}^2}, \quad D^{ij}(\mathbf{k}) = -\frac{4\pi}{k^2}\left(\delta^{ij} - \frac{k^i k^j}{\mathbf{k}^2}\right), \quad D^{0i} = D^{i0} = 0, \tag{13}$$

and $\mathbf{k} = \mathbf{p} - \mathbf{q}$. Here γ_μ and $u(p)$ are the Dirac matrices and spinors

$$u^\lambda(p) = \sqrt{\frac{\epsilon(p) + m}{2\epsilon(p)}}\left(\begin{array}{c}1 \\ \frac{\boldsymbol{\sigma}\mathbf{p}}{\epsilon(p) + m}\end{array}\right)\chi^\lambda, \tag{14}$$

where $\boldsymbol{\sigma}$ and χ^λ are Pauli matrices and spinors and $\epsilon(p) = \sqrt{\mathbf{p}^2 + m^2}$. The effective long-range vector vertex is given by

$$\Gamma_\mu(\mathbf{k}) = \gamma_\mu + \frac{i\kappa}{2m}\sigma_{\mu\nu}k^\nu, \tag{15}$$

where κ is the Pauli interaction constant characterizing the long-range anomalous chromomagnetic moment of quarks. Vector and scalar confining potentials in the nonrelativistic limit reduce to

$$\begin{aligned}V_V(r) &= (1-\varepsilon)(Ar + B), \\ V_S(r) &= \varepsilon(Ar + B),\end{aligned} \tag{16}$$

reproducing

$$V_{\text{conf}}(r) = V_S(r) + V_V(r) = Ar + B, \tag{17}$$

where ε is the mixing coefficient.

The expression for the quasipotential of the heavy quarkonia, expanded in v^2/c^2 can be found in Ref. [19]. The quasipotential for the heavy quark interaction with a light antiquark without employing the nonrelativistic (v/c) expansion for the light quark is given in Ref. [20]. All the parameters of our model like quark masses, parameters of the linear confining potential A and B, mixing coefficient ε and anomalous chromomagnetic quark moment κ are fixed from the analysis of heavy quarkonium masses and radiative decays. The quark masses $m_b = 4.88$ GeV, $m_c = 1.55$ GeV, $m_s = 0.5$ GeV, $m_{u,d} = 0.33$ GeV and the parameters of the linear potential $A = 0.18$ GeV^2 and $B = -0.30$ GeV have the values inherent for quark models. The value of the mixing coefficient of vector and scalar
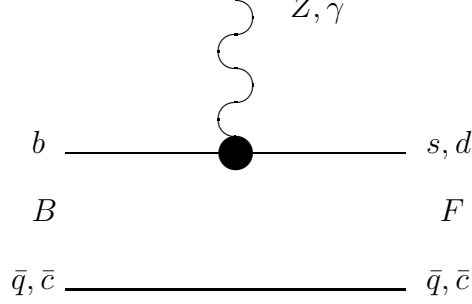
FIG. 1: Lowest order vertex function $\Gamma^{(1)}$ contributing to the current matrix element (18).

confining potentials $\varepsilon = -1$ has been determined from the consideration of the heavy quark expansion for the semileptonic $B \to D$ decays [21] and charmonium radiative decays [19]. Finally, the universal Pauli interaction constant $\kappa = -1$ has been fixed from the analysis of the fine splitting of heavy quarkonia ^3P_J- states [19] and the heavy quark expansion for semileptonic decays of heavy mesons [21] and baryons [28]. Note that the long-range magnetic contribution to the potential in our model is proportional to $(1 + \kappa)$ and thus vanishes for the chosen value of $\kappa = -1$ in accordance with the flux tube model.

IV. MATRIX ELEMENTS OF THE EFFECTIVE WEAK CURRENT OPERATORS FOR $b \to s, d$ TRANSITIONS

In order to calculate the exclusive rare semileptonic decay rate of the B (B_c) meson, it is necessary to determine the corresponding hadronic matrix element of the weak operators (2), (3) between meson states. In the quasipotential approach, the matrix element of the hadronic weak current operator J_μ^W, between a B (B_c) meson with mass M_B and four-momentum p_B and a final meson F $(F = K^{(*)}$ or $D_s^{(*)}$ and $D^{(*)})$ with mass M_F and four-momentum p_F takes the form [29]

$$\langle F(p_F)|J_\mu^W|B(p_B)\rangle = \int \frac{d^3p\,d^3q}{(2\pi)^6} \bar{\Psi}_{F\,\mathbf{p}_F}(\mathbf{p})\Gamma_\mu(\mathbf{p},\mathbf{q})\Psi_{B\,\mathbf{p}_B}(\mathbf{q}), \tag{18}$$

where $\Gamma_\mu(\mathbf{p},\mathbf{q})$ is the two-particle vertex function and $\Psi_{M\,\mathbf{p}_M}$ are the meson $(M = B, F)$ wave functions projected onto the positive energy states of quarks and boosted to the moving reference frame with three-momentum $\mathbf{p}_M$.

The contributions to Γ come from Figs. 1 and 2. The leading order vertex function $\Gamma^{(1)}$ corresponds to the impulse approximation, while the vertex function $\Gamma^{(2)}$ accounts for contributions of the negative-energy states. Note that the form of the relativistic corrections resulting from the vertex function $\Gamma^{(2)}$ is explicitly dependent on the Lorentz structure of the quark-antiquark interaction. In the leading order of the the heavy quark $(m_{b,c} \to \infty)$ and large energy expansions for $B \to F$ transitions, only $\Gamma^{(1)}$ contributes, while $\Gamma^{(2)}$ contributes already at the subleading order. The vertex functions are determined by

$$\Gamma_\mu^{(1)}(\mathbf{p},\mathbf{q}) = \bar{u}_f(p_f)\mathcal{G}_\mu u_b(q_b)(2\pi)^3\delta(\mathbf{p}_q - \mathbf{q}_q), \tag{19}$$

and

$$\Gamma_\mu^{(2)}(\mathbf{p},\mathbf{q}) = \bar{u}_f(p_f)\bar{u}_q(p_q)\Big\{\mathcal{G}_{1\mu}\frac{\Lambda_b^{(-)}(k)}{\epsilon_b(k) + \epsilon_b(p_q)}\gamma_1^0\mathcal{V}(\mathbf{p}_q - \mathbf{q}_q)$$
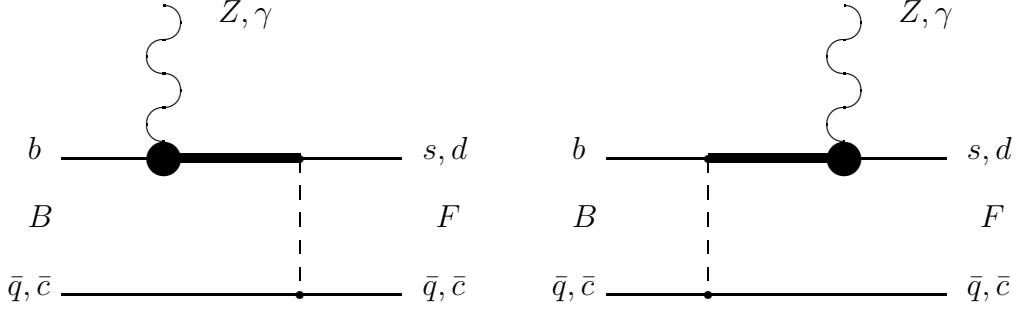
FIG. 2: Vertex function $\Gamma^{(2)}$ taking the quark interaction into account. Dashed lines correspond to the effective potential $\mathcal{V}$ in (12). Bold lines denote the negative-energy part of the quark propagator.

$$+\mathcal{V}(\mathbf{p}_q - \mathbf{q}_q)\frac{\Lambda_f^{(-)}(k')}{\epsilon_f(k') + \epsilon_f(q_f)}\gamma_1^0\mathcal{G}_{1\mu}\Big\}u_b(q_b)u_q(q_q), \tag{20}$$

where $\mathcal{G}_\mu = \gamma_\mu(1 - \gamma_5)$ for the (axial) vector weak current and $\mathcal{G}_\mu = \sigma_{\mu\nu}q^\nu(1 + \gamma_5)$ for the (pseudo) tensor current; the subscripts f and q denote the final active s, d and the spectator u, d, c quarks, respectively; the superscripts "(1)" and "(2)" correspond to Figs. 1 and 2, $\mathbf{k} = \mathbf{p}_f - \boldsymbol{\Delta}$; $\mathbf{k}' = \mathbf{q}_b + \boldsymbol{\Delta}$; $\boldsymbol{\Delta} = \mathbf{p}_F - \mathbf{p}_B$;

$$\Lambda^{(-)}(p) = \frac{\epsilon(p) - (m\gamma^0 + \gamma^0(\boldsymbol{\gamma}\mathbf{p}))}{2\epsilon(p)}.$$

Here [29]

$$p_{f,q} = \epsilon_{f,q}(p)\frac{p_F}{M_F} \pm \sum_{i=1}^{3} n^{(i)}(p_F)p^i,$$

$$q_{b,q} = \epsilon_{b,q}(q)\frac{p_B}{M_B} \pm \sum_{i=1}^{3} n^{(i)}(p_B)q^i,$$

and $n^{(i)}$ are three four-vectors given by

$$n^{(i)\mu}(p) = \left\{\frac{p^i}{M}, \ \delta_{ij} + \frac{p^i p^j}{M(E + M)}\right\}, \quad E = \sqrt{\mathbf{p}^2 + M^2}.$$

It is important to note that the wave functions entering the weak current matrix element (18) are not in the rest frame in general. For example, in the B meson rest frame ($\mathbf{p}_B = 0$), the final meson is moving with the recoil momentum $\boldsymbol{\Delta}$. The wave function of the moving meson $\Psi_{F\boldsymbol{\Delta}}$ is connected with the wave function in the rest frame $\Psi_{F\mathbf{0}} \equiv \Psi_F$ by the transformation [29]

$$\Psi_{F\boldsymbol{\Delta}}(\mathbf{p}) = D_f^{1/2}(R_{L_{\boldsymbol{\Delta}}}^W)D_q^{1/2}(R_{L_{\boldsymbol{\Delta}}}^W)\Psi_{F\mathbf{0}}(\mathbf{p}), \tag{21}$$

where R^W is the Wigner rotation, $L_{\boldsymbol{\Delta}}$ is the Lorentz boost from the meson rest frame to a moving one, and the rotation matrix $D^{1/2}(R)$ in spinor representation is given by

$$\begin{pmatrix} 1 & 0 \\ 0 & 1 \end{pmatrix}D_{q,f}^{1/2}(R_{L_{\boldsymbol{\Delta}}}^W) = S^{-1}(\mathbf{p}_{q,f})S(\boldsymbol{\Delta})S(\mathbf{p}), \tag{22}$$

where

$$S(\mathbf{p}) = \sqrt{\frac{\epsilon(p) + m}{2m}} \left(1 + \frac{\boldsymbol{\alpha}\mathbf{p}}{\epsilon(p) + m}\right)$$

is the usual Lorentz transformation matrix of the four-spinor.

V. FORM FACTORS OF RARE SEMILEPTONIC DECAYS

The matrix elements of the weak current for rare B decays (B denotes either B or B_c) to pseudoscalar mesons ($P = K, D_s, D$) can be parametrized by three invariant form factors,

$$\langle P(p_F)|\bar{q}\gamma^\mu b|B(p_B)\rangle = f_+(q^2)\left[p_B^\mu + p_F^\mu - \frac{M_B^2 - M_P^2}{q^2}\,q^\mu\right] + f_0(q^2)\frac{M_B^2 - M_P^2}{q^2}\,q^\mu, \quad (23)$$

$$\langle P(p_F)|\bar{q}\sigma^{\mu\nu}q_\nu b|B(p_B)\rangle = \frac{if_T(q^2)}{M_B + M_P}[q^2(p_B^\mu + p_F^\mu) - (M_B^2 - M_P^2)q^\mu], \quad (24)$$

where $f_+(0) = f_0(0)$, $q = p_B - p_F$, and $M_{B,P}$ are the masses of the B meson and pseudoscalar P meson, respectively.

The corresponding matrix elements for the rare B decays to vector mesons ($V = K^*, D_s^*, D^*$) are parametrized by seven form factors,

$$\langle V(p_F)|\bar{q}\gamma^\mu b|B(p_B)\rangle = \frac{2iV(q^2)}{M_B + M_V}\epsilon^{\mu\nu\rho\sigma}\epsilon_\nu^* p_{B\rho}p_{F\sigma}, \quad (25)$$

$$\langle V(p_F)|\bar{q}\gamma^\mu\gamma_5 b|B(p_B)\rangle = 2M_V A_0(q^2)\frac{\epsilon^* \cdot q}{q^2}\,q^\mu + (M_B + M_V)A_1(q^2)\left(\epsilon^{*\mu} - \frac{\epsilon^* \cdot q}{q^2}\,q^\mu\right)$$

$$-A_2(q^2)\frac{\epsilon^* \cdot q}{M_B + M_V}\left[p_B^\mu + p_F^\mu - \frac{M_B^2 - M_V^2}{q^2}\,q^\mu\right], \quad (26)$$

$$\langle V(p_F)|\bar{q}i\sigma^{\mu\nu}q_\nu b|B(p_B)\rangle = 2T_1(q^2)\epsilon^{\mu\nu\rho\sigma}\epsilon_\nu^* p_{F\rho}p_{B\sigma}, \quad (27)$$

$$\langle V(p_F)|\bar{q}i\sigma^{\mu\nu}\gamma_5 q_\nu b|B(p_B)\rangle = T_2(q^2)[(M_B^2 - M_V^2)\epsilon^{*\mu} - (\epsilon^* \cdot q)(p_B^\mu + p_F^\mu)]$$

$$+T_3(q^2)(\epsilon^* \cdot q)\left[q^\mu - \frac{q^2}{M_B^2 - M_V^2}(p_B^\mu + p_F^\mu)\right], \quad (28)$$

where $2M_V A_0(0) = (M_B + M_V)A_1(0) - (M_B - M_V)A_2(0)$, $T_1(0) = T_2(0)$; M_V and ϵ_μ are the mass and polarization vector of the final vector meson.

We previously studied the form factors ($f_+, f_0, V, A_0, A_1, A_2$) parametrizing the matrix elements of vector and axial vector charged weak currents for $B \to \pi(\rho)$ [15] and $B_c \to \eta_c(J/\psi)$, $B_c \to D^{(*)}$ [16], $B_c \to B_s^{(*)}(B^{(*)})$ [17] transitions in the framework of our model. The necessary formulas for these form factors can be found in Appendix of Ref. [16]. Now we apply them to the calculation of the form factors, parametrizing neutral current matrix elements for the $B \to K^{(*)}$ and $B_c \to D_s^{(*)}$, $B_c \to D^{(*)}$ transitions. For the remaining tensor form factors we use the same approach described in detail in Refs. [15–17]. Namely, we calculate exactly the contribution of the leading vertex function $\Gamma^{(1)}$ (19) to the transition matrix element of the weak current (18) using the δ-function. For the evaluation of the subleading contribution $\Gamma^{(2)}$ we use expansions in inverse powers of the heavy b-quark mass from the

TABLE I: Form factors of the rare semileptonic decays $B \to K^{(*)}l^+l^-$ calculated in our model. Form factors $f_+(q^2)$, $f_T(q^2)$, $V(q^2)$, $A_0(q^2)$, $T_1(q^2)$ are fitted by Eq. (29), and form factors $f_0(q^2)$, $A_1(q^2)$, $A_2(q^2)$, $T_2(q^2)$, $T_3(q^2)$ are fitted by Eq. (30).

	$B \to K$			$B \to K^*$						
	f_+	f_0	f_T	V	A_0	A_1	A_2	T_1	T_2	T_3
$F(0)$	0.242	0.242	0.258	0.375	0.297	0.321	0.345	0.291	0.291	0.080
σ_1	0.480	0.445	1.198	1.019	0.695	0.374	1.422	0.275	0.855	1.982
σ_2	-0.537	-0.476	2.168	0.229	0.322	-0.138	0.548	-0.339	-0.256	1.198

initial B meson and of the large recoil energy of the final heavy-light meson. Note that the latter contributions turn out to be rather small numerically. Therefore we obtain reliable expressions for the form factors in the whole accessible kinimatical range. It is important to emphasize that doing these calculations we consistently take into account all relativistic corrections including boosts of the meson wave functions from the rest frame to the moving one, given by Eq. (21). The obtained expressions for the tensor form factors f_T, T_1, T_2, T_3 are presented in Appendix (to simplify these expressions the long-range anomalous chromo-magnetic quark moment was explicitly set as $\kappa = -1$). In the limits of the infinitely heavy quark mass and large energy of the final meson, the form factors in our model satisfy all model independent symmetry relations [4, 22].

For numerical calculations of the form factors we use the quasipotential wave functions of the B, B_c, K^*, D_s and D mesons obtained in their mass spectra calculations [19, 20]. Our results for the masses of these mesons are in good agreement with experimental data [30], which we use in our calculations.

We find that the rare semileptonic $B \to K^{(*)}l^+l^-$ and $B_c \to D_s^{(*)}(D^{(*)})l^+l^-$ decay form factors can be approximated with good accuracy by the following expressions [15, 31]:

(a) $F(q^2) = \{f_+(q^2), f_T(q^2), V(q^2), A_0(q^2), T_1(q^2)\}$

$$F(q^2) = \frac{F(0)}{\left(1 - \frac{q^2}{\tilde{M}^2}\right)\left(1 - \sigma_1 \frac{q^2}{M_{B_s^*}^2} + \sigma_2 \frac{q^4}{M_{B_s^*}^4}\right)},\qquad(29)$$

(b) $F(q^2) = \{f_0(q^2), A_1(q^2), A_2(q^2), T_2(q^2), T_3(q^2)\}$

$$F(q^2) = \frac{F(0)}{\left(1 - \sigma_1 \frac{q^2}{M_{B_s^*}^2} + \sigma_2 \frac{q^4}{M_{B_s^*}^4}\right)},\qquad(30)$$

where $\tilde{M} = M_{B_s}$ for A_0 and $\tilde{M} = M_{B_s^*}$ for all other form factors (for $B_c \to D^{(*)}l^+l^-$ decays $M_{B_s^{(*)}}$ should be replaced by $M_{B^{(*)}}$). The values $F(0)$ and $\sigma_{1,2}$ are given in Tables I-III. The difference of fitted form factors from the calculated ones does not exceed 1%. We plot these form factors in Figs. 3 and 4.

VI. RESULTS AND DISCUSSION

Now we use the obtained form factors for the numerical calculation of decay rates and other important observables of the rare semileptonic B decays and confront their values with

TABLE II: Form factors of the rare semileptonic decays $B_c \to D_s^{(*)} l^+ l^-$ calculated in our model. Form factors $f_+(q^2)$, $f_T(q^2)$, $V(q^2)$, $A_0(q^2)$, $T_1(q^2)$ are fitted by Eq. (29), and form factors $f_0(q^2)$, $A_1(q^2)$, $A_2(q^2)$, $T_2(q^2)$, $T_3(q^2)$ are fitted by Eq. (30).

	$B_c \to D_s$			$B_c \to D_s^*$						
	f_+	f_0	f_T	V	A_0	A_1	A_2	T_1	T_2	T_3
$F(0)$	0.129	0.129	0.098	0.182	0.070	0.089	0.110	0.085	0.085	0.051
σ_1	2.096	2.331	1.412	2.133	1.561	2.479	2.833	1.540	2.577	2.783
σ_2	1.147	1.666	0.048	1.183	0.192	1.686	2.167	0.248	1.859	2.170

TABLE III: Form factors of the rare semileptonic decays $B_c \to D^{(*)} l^+ l^-$ calculated in our model. Form factors $f_+(q^2)$, $f_T(q^2)$, $V(q^2)$, $A_0(q^2)$, $T_1(q^2)$ are fitted by Eq. (29), and form factors $f_0(q^2)$, $A_1(q^2)$, $A_2(q^2)$, $T_2(q^2)$, $T_3(q^2)$ are fitted by Eq. (30).

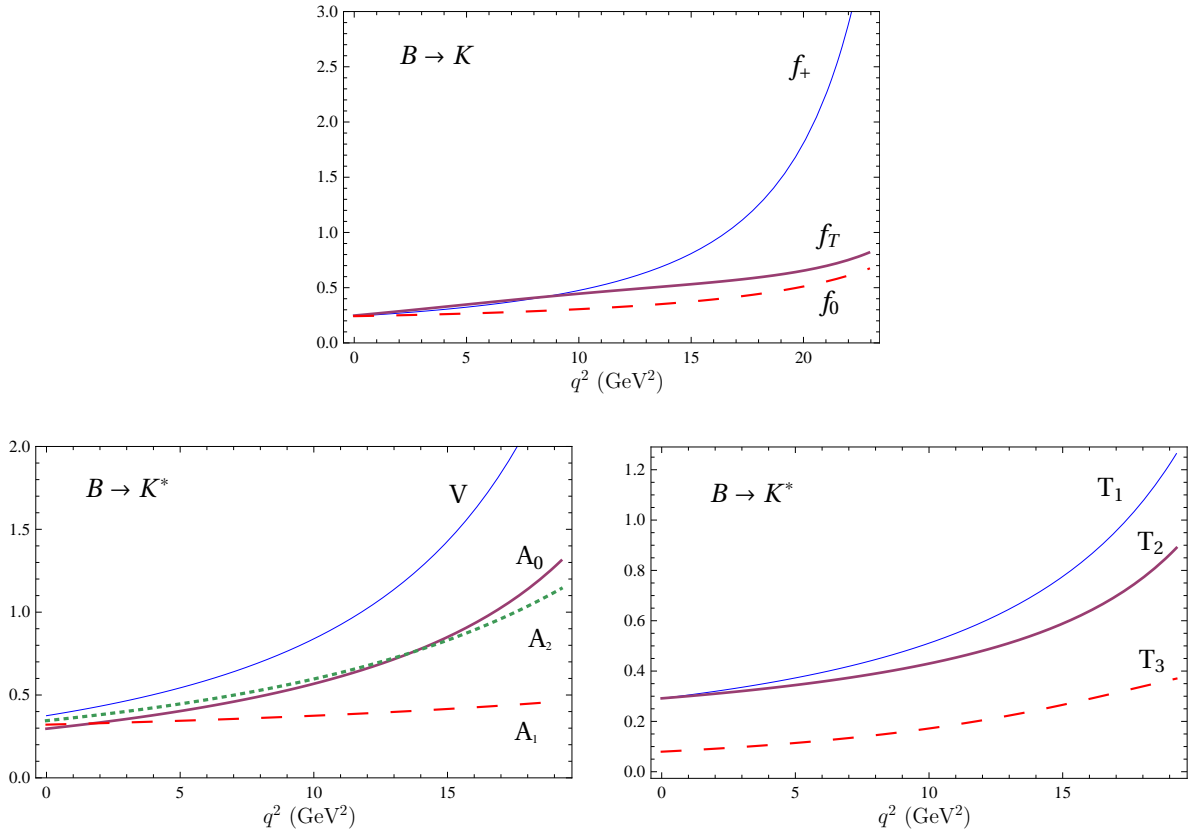|	$B_c \to D$			$B_c \to D^*$						
	f_+	f_0	f_T	V	A_0	A_1	A_2	T_1	T_2	T_3
$F(0)$	0.081	0.081	0.061	0.125	0.035	0.054	0.071	0.055	0.055	0.034
σ_1	2.167	2.455	1.363	2.247	1.511	2.595	2.800	1.520	2.633	2.801
σ_2	1.203	1.729	0.026	1.346	0.175	1.784	2.073	0.207	1.886	2.108

FIG. 3: Form factors of the $B \to K^{(*)}$ decays.
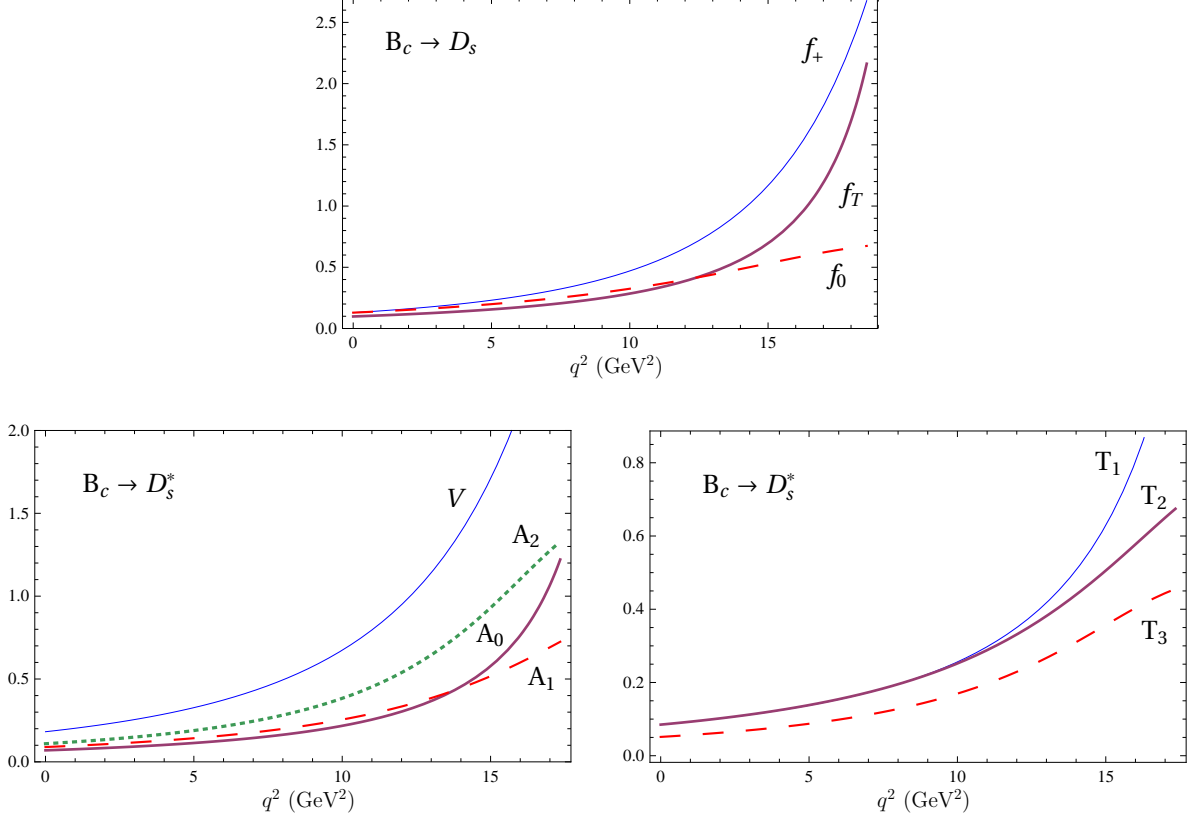
FIG. 4: Form factors of the $B_c \to D_s^{(*)}$ decays.

available experimental data.

A. $B \to P l^+ l^-$ and $B \to V l^+ l^-$ decays

The matrix element of the $b \to f l^+ l^-$ ($f = s$ or d) decay amplitude (4) between meson states can be written [11, 25] in the following form

$$\mathcal{M}(B \to P l^+ l^-) = \frac{G_F \alpha}{2\sqrt{2}\pi}|V_{tf}^* V_{tb}| \left[T_\mu^{(1)}(\bar{l}\gamma^\mu l) + T_\mu^{(2)}(\bar{l}\gamma^\mu \gamma_5 l) \right],$$

$$\mathcal{M}(B \to V l^+ l^-) = \frac{G_F \alpha}{2\sqrt{2}\pi}|V_{tf}^* V_{tb}| \left[\epsilon^{\dagger\nu} T_{\mu\nu}^{(1)}(\bar{l}\gamma^\mu l) + \epsilon^{\dagger\nu} T_{\mu\nu}^{(2)}(\bar{l}\gamma^\mu \gamma_5 l) \right], \quad (31)$$

where $T^{(i)}$ are expressed through the form factors and the Wilson coefficients. Then these amplitudes can be written in the helicity basis $\varepsilon^\mu(m)$ as (see [11])
(a) $B \to P$ transition:

$$H_m^{(i)} = \varepsilon^{\dagger\mu}(m) T_\mu^{(i)}, \quad (32)$$

where

$$H_\pm^{(i)} = 0,$$

$$H_0^{(1)} = \frac{\lambda^{1/2}}{\sqrt{q^2}} \left[C_9^{eff} f_+(q^2) + C_7^{eff} \frac{2m_b}{M_B + M_P} f_T(q^2) \right],$$

$$H_0^{(2)} = \frac{\lambda^{1/2}}{\sqrt{q^2}}C_{10}f_+(q^2),$$

$$H_t^{(1)} = \frac{M_B^2 - M_P^2}{\sqrt{q^2}}C_9^{eff}f_0(q^2),$$

$$H_t^{(2)} = \frac{M_B^2 - M_P^2}{\sqrt{q^2}}C_{10}f_0(q^2). \tag{33}$$

Here $\lambda \equiv \lambda(M_B^2, M_P^2, q^2) = M_B^4 + M_P^4 + q^4 - 2(M_B^2 M_P^2 + M_P^2 q^2 + M_B^2 q^2)$ and the subscripts $\pm, 0, t$ denote transverse, longitudinal and time helicity components, respectively.

(b) $B \to V$ transition:

$$H_m^{(i)} = \varepsilon^{\dagger\mu}(m)\epsilon^{\dagger\nu}T_{\mu\nu}^{(i)}, \tag{34}$$

where ϵ^ν is the polarization vector of the vector V meson and

$$H_\pm^{(1)} = -(M_B^2 - M_V^2)\left[C_9^{eff}\frac{A_1(q^2)}{M_B - M_V} + \frac{2m_b}{q^2}C_7^{eff}T_2(q^2)\right]$$
$$\pm\lambda^{1/2}\left[C_9^{eff}\frac{V(q^2)}{M_B + M_V} + \frac{2m_b}{q^2}C_7^{eff}T_1(q^2)\right],$$

$$H_\pm^{(2)} = C_{10}\left[-(M_B + M_V)A_1(q^2) \pm \lambda^{1/2}\frac{V(q^2)}{M_B + M_V}\right],$$

$$H_0^{(1)} = -\frac{1}{2M_V\sqrt{q^2}}\left[C_9^{eff}\left\{(M_B^2 - M_V^2 - q^2)(M_B + M_V)A_1(q^2) - \frac{\lambda}{M_B + M_V}A_2(q^2)\right\}\right.$$
$$\left.+2m_bC_7^{eff}\left\{(M_B^2 + 3M_V^2 - q^2)T_2(q^2) - \frac{\lambda}{M_B^2 - M_V^2}T_3(q^2)\right\}\right],$$

$$H_0^{(2)} = -\frac{1}{2M_V\sqrt{q^2}}C_{10}\left[(M_B^2 - M_V^2 - q^2)(M_B + M_V)A_1(q^2) - \frac{\lambda}{M_B + M_V}A_2(q^2)\right],$$

$$H_t^{(1)} = -\frac{\lambda^{1/2}}{\sqrt{q^2}}C_9^{eff}A_0(q^2),$$

$$H_t^{(2)} = -\frac{\lambda^{1/2}}{\sqrt{q^2}}C_{10}A_0(q^2), \tag{35}$$

here $\lambda \equiv \lambda(M_B^2, M_V^2, q^2) = M_B^4 + M_V^4 + q^4 - 2(M_B^2 M_V^2 + M_V^2 q^2 + M_B^2 q^2)$.

The differential decay rate then reads [11]

$$\frac{d\Gamma(B \to P(V)l^+l^-)}{dq^2} = \frac{G_F^2}{(2\pi)^3}\left(\frac{\alpha|V_{tf}^* V_{tb}|}{2\pi}\right)^2\frac{\lambda^{1/2}q^2}{48M_B^3}\sqrt{1 - \frac{4m_l^2}{q^2}}\left[H^{(1)}H^{\dagger(1)}\left(1 + \frac{4m_l^2}{q^2}\right)\right.$$
$$\left.+H^{(2)}H^{\dagger(2)}\left(1 - \frac{4m_l^2}{q^2}\right) + \frac{2m_l^2}{q^2}3H_t^{(2)}H_t^{\dagger(2)}\right], \tag{36}$$

where m_l is the lepton mass and

$$H^{(i)}H^{\dagger(i)} \equiv H_+^{(i)}H_+^{\dagger(i)} + H_-^{(i)}H_-^{\dagger(i)} + H_0^{(i)}H_0^{\dagger(i)}. \tag{37}$$

The forward-backward asymmetry is given by

$$A_{FB} = \frac{3}{4}\sqrt{1 - \frac{4m_l^2}{q^2}}\frac{\text{Re}(H_+^{(1)}H_+^{\dagger(2)}) - \text{Re}(H_-^{(1)}H_-^{\dagger(2)})}{H^{(1)}H^{\dagger(1)}\left(1 + \frac{4m_l^2}{q^2}\right) + H^{(2)}H^{\dagger(2)}\left(1 - \frac{4m_l^2}{q^2}\right) + \frac{2m_l^2}{q^2}3H_t^{(2)}H_t^{\dagger(2)}}. \tag{38}$$

The longitudinal fraction of the V polarization has the form

$$F_L = \frac{H_0^{(1)} H_0^{\dagger(1)} \left(1 + \frac{4m_l^2}{q^2}\right) + H_0^{(2)} H_0^{\dagger(2)} \left(1 - \frac{4m_l^2}{q^2}\right) + \frac{2m_l^2}{q^2} 3 H_t^{(2)} H_t^{\dagger(2)}}{H^{(1)} H^{\dagger(1)} \left(1 + \frac{4m_l^2}{q^2}\right) + H^{(2)} H^{\dagger(2)} \left(1 - \frac{4m_l^2}{q^2}\right) + \frac{2m_l^2}{q^2} 3 H_t^{(2)} H_t^{\dagger(2)}}. \tag{39}$$

These two observables are the most popular quantities for $B \to K^*(\to K\pi)\mu^+\mu^-$ decays, since they are convenient for the experimental measurements. They enter the decay differential distributions in $\cos\theta_K$

$$\frac{1}{\Gamma}\frac{d\Gamma(B \to K^*\mu^+\mu^-)}{d\cos\theta_K} = \frac{3}{2}F_L \cos^2\theta_K + \frac{3}{4}(1 - F_L)(1 - \cos^2\theta_K), \tag{40}$$

and in $\cos\theta_\mu$

$$\frac{1}{\Gamma}\frac{d\Gamma(B \to K^*\mu^+\mu^-)}{d\cos\theta_\mu} = \frac{3}{4}F_L(1 - \cos^2\theta_\mu) + \frac{3}{8}(1 - F_L)(1 + \cos^2\theta_\mu) + A_{FB}\cos\theta_\mu, \tag{41}$$

where θ_K is the angle between the kaon direction and the direction opposite to the B meson in the K^* rest frame, and θ_μ is the angle between the μ^+ and the opposite of the B direction in the dilepton rest frame. Therefore they can be determined experimentally using the angular analysis.

B. $B \to P\nu\bar{\nu}$ and $B \to V\nu\bar{\nu}$ decays

The differential decay rate for the $B \to P(V)\nu\bar{\nu}$ is given by

$$\frac{d\Gamma(B \to P(V)\nu\bar{\nu})}{dq^2} = 3\frac{G_F^2}{(2\pi)^3}\left(\frac{\alpha|V_{tf}^* V_{tb}|}{2\pi}\right)^2 \frac{\lambda^{1/2}q^2}{24M_B^3} H^{(\nu)} H^{\dagger(\nu)}, \tag{42}$$

where the factor of 3 originates from the sum over neutrino flavours,

$$H^{(\nu)} H^{\dagger(\nu)} \equiv H_+^{(\nu)} H_+^{\dagger(\nu)} + H_-^{(\nu)} H_-^{\dagger(\nu)} + H_0^{(\nu)} H_0^{\dagger(\nu)},$$

and the helicty amplitudes $H_m^{(\nu)}$ read as follows
(a) $B \to P$ transition:

$$\begin{aligned} H_\pm^{(\nu)} &= 0, \\ H_0^{(\nu)} &= \frac{\lambda^{1/2}}{\sqrt{q^2}}C_L^\nu f_+(q^2). \end{aligned} \tag{43}$$

(b) $B \to V$ transition:

$$\begin{aligned} H_\pm^{(\nu)} &= C_L^\nu\left[-(M_B + M_V)A_1(q^2) \pm \lambda^{1/2}\frac{V(q^2)}{M_B + M_V}\right], \\ H_0^{(\nu)} &= -\frac{1}{2M_V\sqrt{q^2}}C_L^\nu\left[(M_B^2 - M_V^2 - q^2)(M_B + M_V)A_1(q^2) - \frac{\lambda}{M_B + M_V}A_2(q^2)\right]. \end{aligned} \tag{44}$$

TABLE IV: Comparison of our predictions for the rare semileptonic $B \to K^{(*)}$ decay nonresonant branching fractions with experimental data (in 10^{-7}).

Decay	our	BaBar [6, 33]	Belle [7, 34]	CDF [8]	CDF [9]	HFAG [35]
$B \to K\mu^+\mu^-$	4.19	$3.4 \pm 0.7 \pm 0.2$	$4.8^{+0.5}_{-0.4} \pm 0.3$	$5.9 \pm 1.5 \pm 0.4$	$3.8 \pm 0.5 \pm 0.3$	4.5 ± 0.4
$B \to K\tau^+\tau^-$	1.17					
$B \to K\nu\bar{\nu}$	26.1		< 140			
$B \to K^*\mu^+\mu^-$	9.25	$7.8^{+1.9}_{-1.7} \pm 1.1$	$10.7^{+1.1}_{-1.0} \pm 0.9$	$8.1 \pm 3.0 \pm 1.0$	$10.6 \pm 1.4 \pm 0.9$	$10.8^{+1.2}_{-1.1}$
$B \to K^*\tau^+\tau^-$	1.03					
$B \to K^*\nu\bar{\nu}$	63.2	< 800				

Here $C_L^\nu = -X(x_t)/\sin^2\theta_W$, with $x_t = m_t^2/m_W^2$, θ_W is the Weinberg angle, and the function $X(x_t)$ at the leading-order in QCD has the form

$$X(x_t) = \frac{x}{8}\left(\frac{2+x}{x-1} + \frac{3x-6}{(x-1)^2}\ln x\right),$$

while the next-to-leading order expressions are given in Ref. [32].

Substituting the current experimental values for the top (m_t) and W-boson (m_W) masses one gets [2]

$$C_L^\nu = -6.38 \pm 0.06, \tag{45}$$

where the error is dominated by the top quark mass uncertainty. In the following calculations we use the central value of C_L^ν.

The differential longitudinal polarization fraction F_L of the V meson is defined similar to Eq. (39)

$$F_L = \frac{H_0^{(\nu)}H_0^{\dagger(\nu)}}{H^{(\nu)}H^{\dagger(\nu)}}. \tag{46}$$

C.   Numerical results

Now we substitute the above calculated form factors in the expressions for decay rates, asymmetries and polarization fractions and perform numerical calculations.

First we compare the predictions of our model for the $B \to Kl^+l^-$ and $B \to K^*l^+l^-$ decays with available experimental data. The calculated values for the branching fractions of the rare semileptonic decays $B \to K^{(*)}l^+l^-$ and $B \to K^{(*)}\nu\bar{\nu}$ and available experimental data are given in Table IV. We find good agreement of our results for the $B \to K\mu^+\mu^-$ and $B \to K^*\mu^+\mu^-$ decays with experimental data. A more stringent test of our predictions can be achieved by comparison with new data on differential decay distributions. This is done in Fig. 5 where we confront our predictions for differential decay rates, the longitudinal polarization fraction F_L of the K^* and the muon forward-backward asymmetry A_{FB} with detailed experimental data from Belle [7] and CDF [9]. In this figure we plot our results both for the nonresonant (solid line) quantities and quantities including the J/ψ and ψ' resonance contributions (dashed line). Note that the resonance regions are vetoed in the experimental analysis. Reasonable agreement of our predictions with experimental data is found. The current experimental data on A_{FB} are not precise enough to give a definite
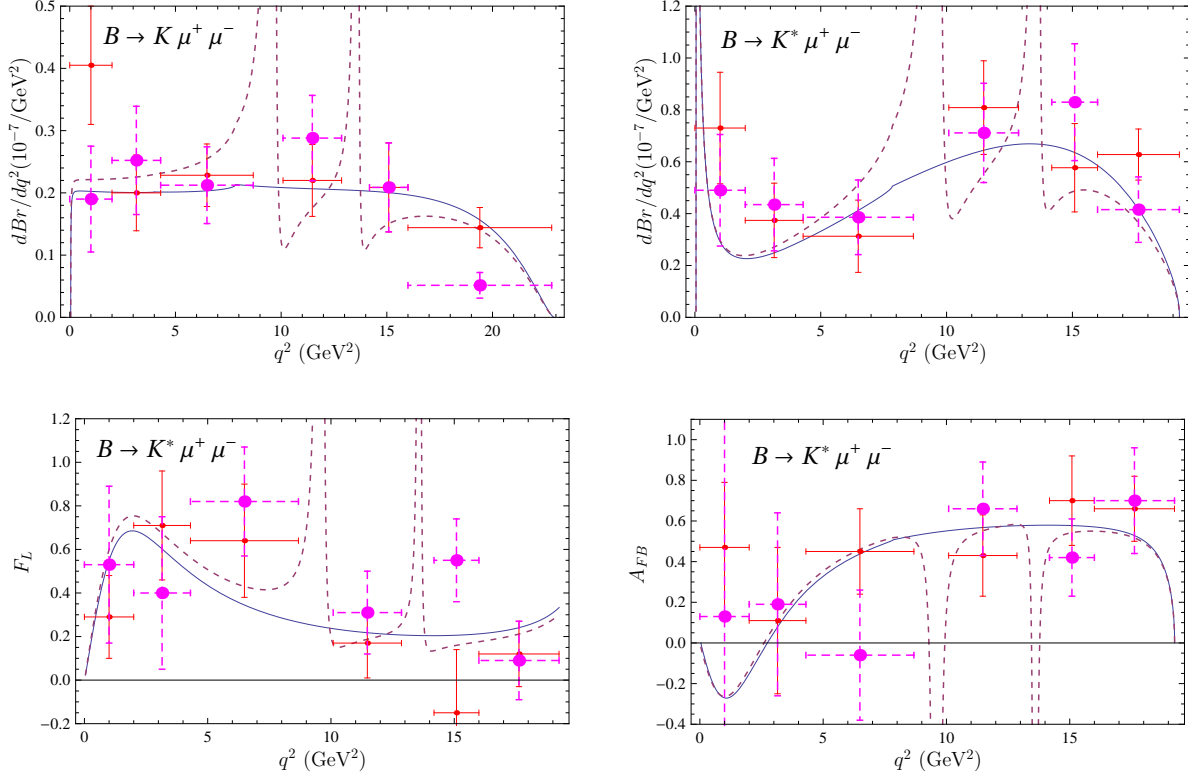
FIG. 5: Comparison of theoretical predictions for the differential branching fractions dBr/dq^2, the K^* longitudinal polarization F_L and muon forward-backward asymmetry A_{FB} for $B \to K^{(*)}$ decays with available experimental data. Nonresonant and resonant results are plotted by solid and dashed lines, respectively. Belle data are given by dots with solid error bars, while CDF data are presented by filled circles with dashed error bars.

conclusion whether this asymmetry has a zero or not. Our model predicts the zero of A_{FB} at $q_0^2 = 2.74$ GeV^2 which is in agreement with the value $q_0^2 = 2.88^{+0.44}_{-0.28}$ GeV^2 given in [25]. It is expected that the accuracy of experimental data will increase significantly in the near future.

In Fig. 6 we plot our results for the differential branching fractions of the $B \to K\tau^+\tau^-$ and $B \to K^*\tau^+\tau^-$ decays. The calculated values for these decay branching fractions are presented in Table IV. There we also give our results for the $B \to K\nu\bar{\nu}$ and $B \to K^*\nu\bar{\nu}$ branching fractions. None of these modes have been measured yet. Only experimental upper bounds have been recently set on branching fractions for the $B \to K^*\nu\bar{\nu}$ decay by BaBar [33] and for the $B \to K\nu\bar{\nu}$ decay by Belle [34]. These bounds are about an order of magnitude higher than our model predictions. In Fig. 7 we show our predictions for the differential branching fraction and the K^* longitudinal polarization fraction F_L for the $B \to K^*\nu\bar{\nu}$ decay. As it is noted in Ref. [2], the value $F_L(0) = 1$ is imposed by helicity conservation, while $F_L(q_{max}^2) = 1/3$ follows from the absence of a preferential direction at the point $q_{max}^2 = (M_B - M_{K^*})^2$ where both K^* and B are at rest. The differential branching fraction of the $B \to K^*\nu\bar{\nu}$ decay as well as its integrated value are close to the ones $(Br(B \to K^*\nu\bar{\nu}) = (6.8^{+1.0}_{-1.1}) \times 10^{-6})$ given in Ref. [2], while the shape of F_L is slightly different. We also get the value for the q^2 integrated longitudinal polarization fraction $\langle F_L \rangle \approx 0.31$, which is significantly lower than the one of Ref. [2] $\langle F_L \rangle = 0.54 \pm 0.01$. Note
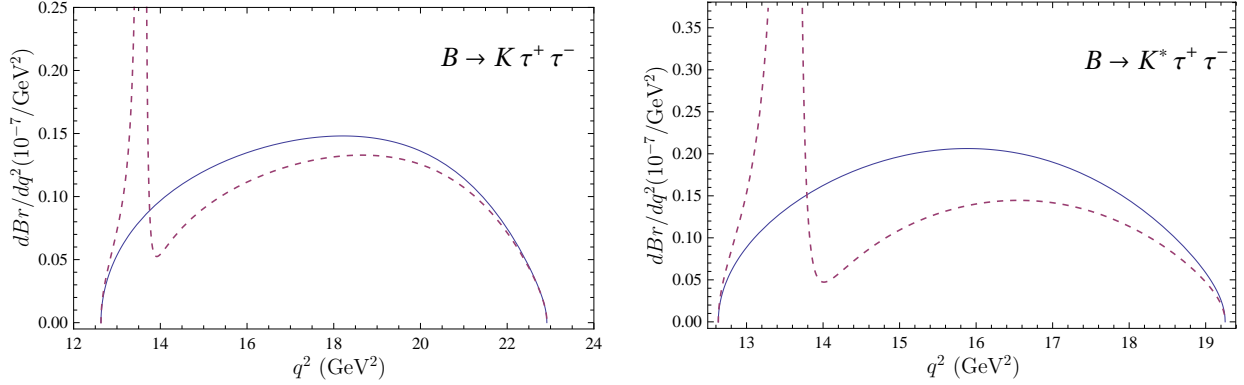
FIG. 6: Predictions for the differential branching fractions of $B \to K^{(*)}\tau^+\tau^-$ decays. Nonresonant and resonant results are plotted by solid and dashed lines, respectively.
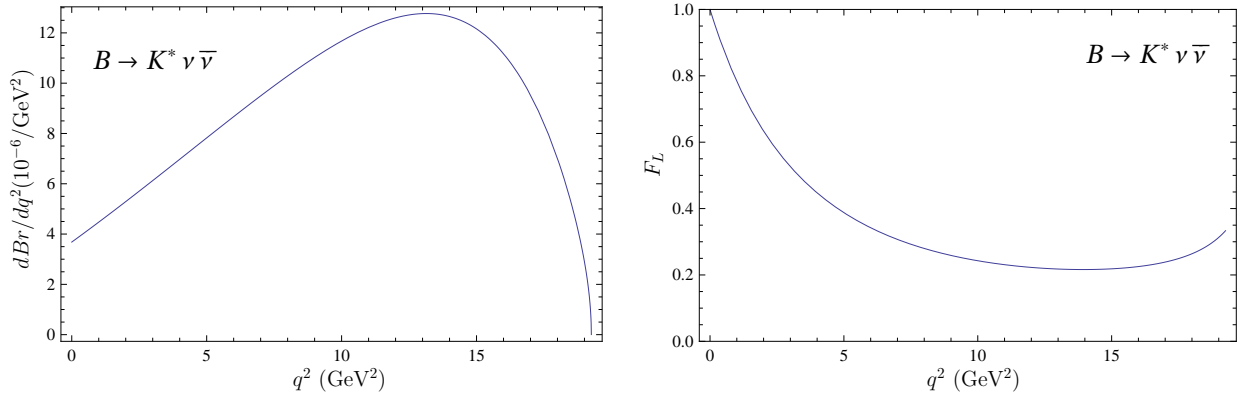

FIG. 7: Predictions for the differential branching fractions and the K^* longitudinal polarization fraction F_L for the $B \to K^*\nu\bar{\nu}$ decay.

that our results for the branching fractions of the $B \to K^{(*)}\nu\bar{\nu}$ decay, though consistent with the ones from [2], are somewhat lower than the predictions from [23, 26].

Next we present our results for the rare semileptonic B_c decays. In Table V we compare available theoretical predictions for the branching fractions of the rare semileptonic $B_c \to D_s^{(*)}$ and $B_c \to D^{(*)}$ decays. The investigations [11–13] are based on the relativistic constituent quark model and light-front quark models, while the authors of Ref. [14] use three-point QCD sum rules. Although the results of these approaches are consistent in the order of magnitude of the branching fractions, they differ by more than a factor of 2 for some decay modes. We find the best overall agreement of our predictions for the branching fractions with the results of the relativistic quark model [11]. The differential branching fractions, the longitudinal polarization F_L of the final vector meson and the muon forward-backward asymmetry A_{FB} for the $B_c \to D_s$ and $B_c \to D_s^*$ transitions in our model are plotted in Figs. 8 and 9. Similar curves have been obtained for $B_c \to D^{(*)}$ transitions and are not shown here. We predict the following values of the position of the zero of the forward-backward asymmetry A_{FB}: $q_0^2 = 2.41$ GeV^2 for the $B_c \to D_s^*\mu^+\mu^-$ decay and $q_0^2 = 2.46$ GeV^2 for the $B_c \to D^*\mu^+\mu^-$ decay.

TABLE V: Comparison of theoretical predictions for the nonresonant branching fractions of the rare semileptonic $B_c \to D_s^{(*)}$ and $B_c \to D^{(*)}$ decays (in 10^{-8}).

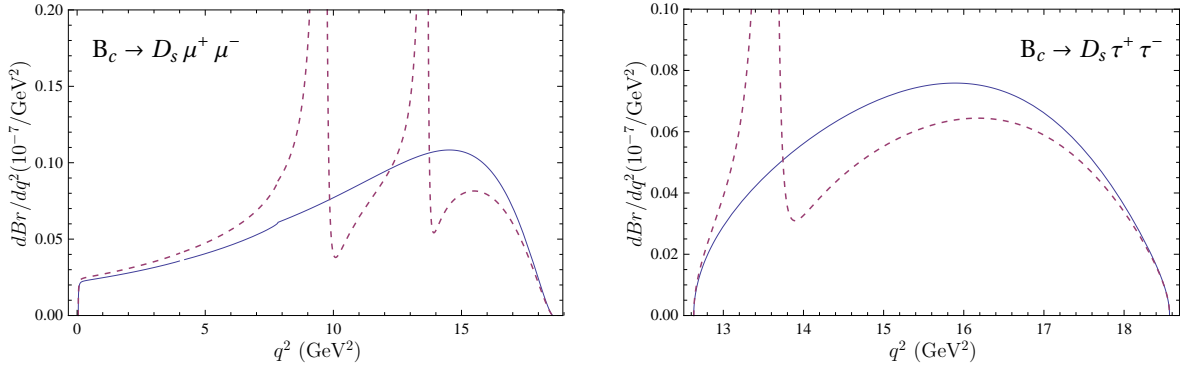| Decay	our	[11]	[12]	[14]	[13]
$B_c \to D_s \mu^+ \mu^-$	11.6	9.7	13.6	6.1 ± 1.5	5.4
$B_c \to D_s \tau^+ \tau^-$	3.3	2.2	3.4	2.3 ± 0.5	1.4
$B_c \to D_s \nu \bar{\nu}$	65	73	92	49 ± 12	39
$B_c \to D_s^* \mu^+ \mu^-$	21.2	17.6	40.9	29.9 ± 5.0	
$B_c \to D_s^* \tau^+ \tau^-$	3.5	2.2	5.1	2.05 ± 0.76	
$B_c \to D_s^* \nu \bar{\nu}$	135	142	312		
$B_c \to D \mu^+ \mu^-$	0.37	0.44	0.41	0.31 ± 0.06	0.18
$B_c \to D \tau^+ \tau^-$	0.15	0.11	0.13	0.13 ± 0.03	0.08
$B_c \to D \nu \bar{\nu}$	2.16	3.28	2.77	3.48 ± 0.71	1.31
$B_c \to D^* \mu^+ \mu^-$	0.81	0.71	1.01	1.58 ± 0.20	
$B_c \to D^* \tau^+ \tau^-$	0.19	0.11	0.18	$0.08 - 0.11$	
$B_c \to D^* \nu \bar{\nu}$	5.12	5.78	7.64		

FIG. 8: Predictions for the differential $B_c \to D_s$ decay branching fractions. Nonresonant and resonant results are plotted by solid and dashed lines, respectively.

VII. CONCLUSIONS

In this paper we obtained the form factors of rare semileptonic decays of the B and B_c mesons in the framework of the QCD-motivated relativistic quark model based on the quasipotential approach. The consideration is done with a systematic account of all relativistic effects, which are very important for such transitions. Particular attention was devoted to the inclusion of negative-energy contributions and to the relativistic transformation of the meson wave function from the rest to the moving reference frame. As a result, the q^2 dependence of these form factors was explicitly determined in the whole accessible kinematical range without using any ad hoc assumptions and extrapolations. It is important to point out that the obtained form factors satisfy all heavy quark and large energy symmetry relations in the corresponding limits [22]. Note that the resulting decay form factors are expressed through the overlap integrals of the initial and final meson wave functions. The relativistic wave functions, obtained previously in the investigations of the meson mass
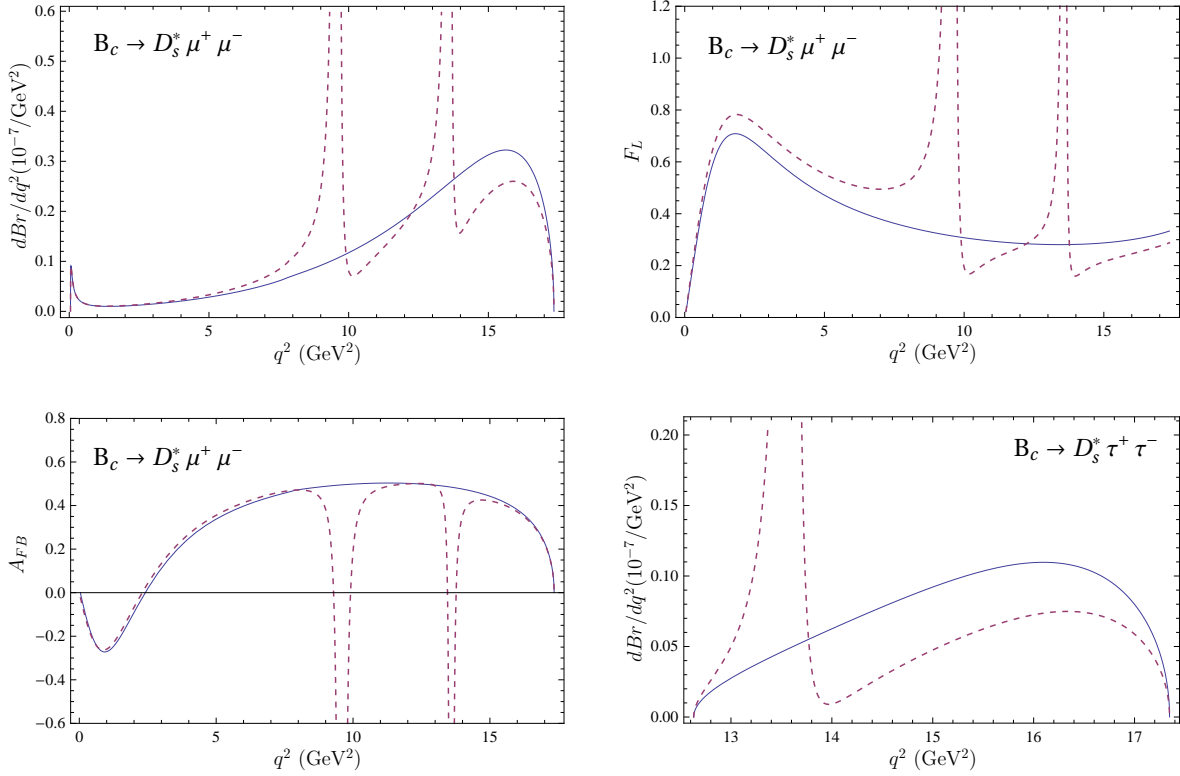
FIG. 9: Predictions for the differential branching fractions dBr/dq^2, the longitudinal polarization F_L and muon forward-backward asymmetry A_{FB} for $B_c \to D_s^*$ decays. Nonresonant and resonant results are plotted by solid and dashed lines, respectively.

spectra, were used for the numerical calculations. This significantly improves the reliability of the calculated form factors. On the basis of these form factors branching fractions and different differential decay distributions were obtained.

First we tested our model by confronting its results for the $B \to K\mu^+\mu^-$ and $B \to K^*\mu^+\mu^-$ decays with the available detailed experimental data. It was found that the total and differential branching fractions, the K^* meson longitudinal polarization fraction F_L and the muon forward-backward asymmetry A_{FB} agree well with data.

Secondly, we presented detailed predictions for the rare semileptonic decays of the B_c meson which can be investigated in the LHCb experiment at CERN, where the B_c mesons are expected to be copiously produced. Finally, we compare our results on these decays with the ones previously available in the literature in Table V. The predictions for the differential branching fractions, the vector meson longitudinal polarization fraction F_L and muon forward-backward asymmetry A_{FB} are also given in Figs. 8 and 9.

Appendix: Tensor form factors of rare B and B_c decays

(a) $B \to P$ ($B \to K$, $B_c \to D_s$ and $B_c \to D$) transitions (see Eq. (24))

$$f_T(q^2) = f_T^{(1)}(q^2) + \varepsilon f_T^{S(2)}(q^2) + (1 - \varepsilon) f_T^{V(2)}(q^2), \tag{A.1}$$

$$
\begin{aligned}
f_T^{(1)}(q^2) =\; & (M_B + M_P)\sqrt{\frac{E_P}{M_B}} \int \frac{d^3 p}{(2\pi)^3} \bar{\Psi}_P\left(\mathbf{p} + \frac{\epsilon_q}{E_P + M_P}\boldsymbol{\Delta}\right) \sqrt{\frac{\epsilon_f(p+\Delta) + m_f}{2\epsilon_f(p+\Delta)}} \sqrt{\frac{\epsilon_b(p) + m_b}{2\epsilon_b(p)}} \\
& \times \left\{ \frac{1}{\epsilon_f(p+\Delta) + m_f} + \frac{(\mathbf{p}\boldsymbol{\Delta})}{\boldsymbol{\Delta}^2}\left(\frac{1}{\epsilon_f(p+\Delta) + m_f} - \frac{1}{\epsilon_b(p) + m_b} \right) \right. \\
& \left. + \frac{2}{3}\frac{\mathbf{p}^2}{E_P + M_P}\left(\frac{1}{\epsilon_f(p+\Delta) + m_f} - \frac{1}{\epsilon_q(p) + m_q} \right) \right. \\
& \left. \times \left(\frac{1}{\epsilon_f(p+\Delta) + m_f} + \frac{1}{\epsilon_b(p) + m_b} \right) \right\} \Psi_B(\mathbf{p}), \tag{A.2}
\end{aligned}
$$

$$
\begin{aligned}
f_T^{S(2)}(q^2) =\; & -(M_B + M_P)\sqrt{\frac{E_P}{M_B}} \int \frac{d^3 p}{(2\pi)^3} \bar{\Psi}_P\left(\mathbf{p} + \frac{2\epsilon_q}{E_P + M_P}\boldsymbol{\Delta}\right) \sqrt{\frac{\epsilon_f(p+\Delta) + m_f}{2\epsilon_f(p+\Delta)}} \\
& \times \left\{ \frac{1}{2\epsilon_f(p+\Delta)(\epsilon_f(p+\Delta) + m_f)} \left(1 + \frac{\epsilon_f(p+\Delta) - m_f}{2m_b}\frac{(\mathbf{p}\boldsymbol{\Delta})}{\boldsymbol{\Delta}^2} \right) \right. \\
& \times \left[M_P - \epsilon_f\left(p + \frac{2\epsilon_q}{E_P + M_P}\Delta\right) - \epsilon_q\left(p + \frac{2\epsilon_q}{E_P + M_P}\Delta\right) \right] \\
& + \frac{(\mathbf{p}\boldsymbol{\Delta})}{\boldsymbol{\Delta}^2}\left[\frac{M_B + M_f - \epsilon_b(p) - \epsilon_q(p) - \epsilon_f\left(p + \frac{2\epsilon_q}{E_P + M_P}\Delta\right) - \epsilon_q\left(p + \frac{2\epsilon_q}{E_P + M_P}\Delta\right)}{2\epsilon_f(p+\Delta)(\epsilon_f(p+\Delta) + m_f)} \right. \\
& \left. \left. + \frac{M_B - M_P - \epsilon_b(p) - \epsilon_q(p) + \epsilon_f\left(p + \frac{2\epsilon_q}{E_P + M_P}\Delta\right) + \epsilon_q\left(p + \frac{2\epsilon_q}{E_P + M_P}\Delta\right)}{2m_b(\epsilon_b(p+\Delta) + m_b)} \right] \right\} \Psi_B(\mathbf{p}), \\
& \tag{A.3}
\end{aligned}
$$

$$
\begin{aligned}
f_T^{V(2)}(q^2) =\; & (M_B + M_P)\sqrt{\frac{E_P}{M_B}} \int \frac{d^3 p}{(2\pi)^3} \bar{\Psi}_P\left(\mathbf{p} + \frac{2\epsilon_q}{E_P + M_P}\boldsymbol{\Delta}\right) \sqrt{\frac{\epsilon_f(p+\Delta) + m_f}{2\epsilon_f(p+\Delta)}} \\
& \times \frac{(\mathbf{p}\boldsymbol{\Delta})}{\boldsymbol{\Delta}^2}\left\{ \frac{M_B - \epsilon_b(p) - \epsilon_q(p)}{2\epsilon_f(p+\Delta)(\epsilon_f(p+\Delta) + m_f)} \right. \\
& + \frac{1}{2m_b}\left(\frac{1}{\epsilon_b(p+\Delta) + m_b} - \frac{\epsilon_f(p+\Delta) - m_f}{2\epsilon_f(p+\Delta)(\epsilon_f(p+\Delta) + m_f)} \right) \\
& \left. \times \left[M_P - \epsilon_f\left(p + \frac{2\epsilon_q}{E_P + M_P}\Delta\right) - \epsilon_q\left(p + \frac{2\epsilon_q}{E_P + M_P}\Delta\right) \right] \right\} \Psi_B(\mathbf{p}), \tag{A.4}
\end{aligned}
$$

where the superscripts "(1)" and "(2)" correspond to Figs. 1 and 2, ε is the mixing coefficient in the confinement potential indicated in Eq. (16) and

$$\Delta \equiv |\boldsymbol{\Delta}| = \sqrt{\frac{(M_B^2 + M_P^2 - q^2)^2}{4M_B^2} - M_P^2},$$

$$E_P = \sqrt{M_P^2 + \boldsymbol{\Delta}^2}, \quad \epsilon_Q(p + a\Delta) = \sqrt{m_Q^2 + (\mathbf{p} + a\boldsymbol{\Delta})^2} \quad (Q = b, c, s, u, d).$$

Here B stands for the B or B_c meson, $P = K, D_s, D$ is the final pseudoscalar meson, $f = s, d$ is the final active quark and $q = u, d, c$ denotes the corresponding spectator quark.

(b) $B \to V$ ($B \to K^*$, $B_c \to D_s^*$ and $B_c \to D^*$) transitions (see Eqs. (27) and (28))

$$T_1(q^2) = T_1^{(1)}(q^2) + \varepsilon T_1^{S(2)}(q^2) + (1 - \varepsilon) T_1^{V(2)}(q^2), \tag{A.5}$$

$$
\begin{aligned}
T_1^{(1)}(q^2) =\ & \sqrt{\frac{E_V}{M_B}} \int \frac{d^3p}{(2\pi)^3} \bar{\Psi}_V \left(\mathbf{p} + \frac{2\epsilon_q}{E_V + M_V}\boldsymbol{\Delta}\right) \sqrt{\frac{\epsilon_f(p+\Delta) + m_f}{2\epsilon_f(p+\Delta)}} \sqrt{\frac{\epsilon_b(p) + m_b}{2\epsilon_b(p)}} \\
& \times \Bigg\{ 1 + \frac{\mathbf{p}^2/3 + (\mathbf{p}\boldsymbol{\Delta})}{(\epsilon_f(p+\Delta) + m_f)(\epsilon_b(p) + m_b)} + \\
& \frac{\mathbf{p}^2\boldsymbol{\Delta}^2}{3(E_V + M_V)(\epsilon_q(p) + m_q)(\epsilon_f(p+\Delta) + m_f)(\epsilon_b(p) + m_b)} \\
& + (M_B - E_V)\Bigg[\frac{1}{\epsilon_f(p+\Delta) + m_f} + \frac{(\mathbf{p}\boldsymbol{\Delta})}{\boldsymbol{\Delta}^2}\left(\frac{1}{\epsilon_f(p+\Delta) + m_f} + \frac{1}{\epsilon_b(p) + m_b}\right) \\
& - \frac{\mathbf{p}^2}{3(E_V + M_V)}\left(\frac{1}{\epsilon_q(p) + m_q}\left(\frac{1}{\epsilon_b(p) + m_b} - \frac{1}{\epsilon_f(p+\Delta) + m_f}\right)\right. \\
& + \left.\frac{2}{(\epsilon_f(p) + m_f)^2}\right)\Bigg]\Bigg\} \Psi_B(\mathbf{p}), \tag{A.6}
\end{aligned}
$$

$$
\begin{aligned}
T_1^{S(2)}(q^2) =\ & \sqrt{\frac{E_V}{M_B}} \int \frac{d^3p}{(2\pi)^3} \bar{\Psi}_V \left(\mathbf{p} + \frac{2\epsilon_q}{E_V + M_V}\boldsymbol{\Delta}\right) \sqrt{\frac{\epsilon_f(p+\Delta) + m_f}{2\epsilon_f(p+\Delta)}} \\
& \times \Bigg\{ \frac{\epsilon_f(p+\Delta) - m_f}{2\epsilon_f(p+\Delta)(\epsilon_f(p+\Delta) + m_f)}\left(1 + \frac{M_B - E_V}{2m_b}\frac{(\mathbf{p}\boldsymbol{\Delta})}{\boldsymbol{\Delta}^2}\right) \\
& \times \left(M_V - \epsilon_f\left(p + \frac{2\epsilon_q}{E_V + M_V}\Delta\right) - \epsilon_q\left(p + \frac{2\epsilon_q}{E_V + M_V}\Delta\right)\right) - (M_B - E_V)\frac{(\mathbf{p}\boldsymbol{\Delta})}{\boldsymbol{\Delta}^2} \\
& \times \left(\frac{M_B + M_V - \epsilon_b(p) - \epsilon_q(p) - \epsilon_f\left(p + \frac{2\epsilon_q}{E_V + M_V}\Delta\right) - \epsilon_q\left(p + \frac{2\epsilon_q}{E_V + M_V}\Delta\right)}{2m_b(\epsilon_b(p+\Delta) + m_b)}\right. \\
& + \left.\frac{M_B - M_V - \epsilon_b(p) - \epsilon_q(p) + \epsilon_f\left(p + \frac{2\epsilon_q}{E_V + M_V}\Delta\right) + \epsilon_q\left(p + \frac{2\epsilon_q}{E_V + M_V}\Delta\right)}{2\epsilon_f(p+\Delta)(\epsilon_f(p+\Delta) + m_f)}\right)\Bigg\} \Psi_B(\mathbf{p}), \\
& \tag{A.7}
\end{aligned}
$$

$$
\begin{aligned}
T_1^{V(2)}(q^2) =\ & \sqrt{\frac{E_V}{M_V}} \int \frac{d^3p}{(2\pi)^3} \bar{\Psi}_V \left(\mathbf{p} + \frac{2\epsilon_q}{E_V + M_V}\boldsymbol{\Delta}\right) \sqrt{\frac{\epsilon_f(p+\Delta) + m_f}{2\epsilon_f(p+\Delta)}} \\
& \times \Bigg\{ \frac{\epsilon_f(p+\Delta) - m_f}{2\epsilon_f(p+\Delta)(\epsilon_f(p+\Delta) + m_f)}\left(1 + \frac{M_B - E_V}{2m_b}\frac{(\mathbf{p}\boldsymbol{\Delta})}{\boldsymbol{\Delta}^2}\right) \\
& \times \left(M_V - \epsilon_f\left(p + \frac{2\epsilon_q}{E_V + M_V}\Delta\right) - \epsilon_q\left(p + \frac{2\epsilon_q}{E_V + M_V}\Delta\right)\right) + (M_B - E_V)\frac{(\mathbf{p}\boldsymbol{\Delta})}{\boldsymbol{\Delta}^2}
\end{aligned}
$$

$$\times\left(\frac{M_V - \epsilon_f\left(p + \frac{2\epsilon_q}{E_V+M_V}\Delta\right) - \epsilon_q\left(p + \frac{2\epsilon_q}{E_V+M_V}\Delta\right)}{2m_b(\epsilon_b(p+\Delta)+m_b)}\right.$$

$$\left.\left.+\frac{M_B - \epsilon_b(p) - \epsilon_q(p)}{2\epsilon_f(p+\Delta)(\epsilon_f(p+\Delta)+m_f)}\right)\right\}\Psi_B(\mathbf{p}), \tag{A.8}$$

$$T_2(q^2) = T_2^{(1)}(q^2) + \varepsilon T_2^{S(2)}(q^2) + (1-\varepsilon)T_2^{V(2)}(q^2), \tag{A.9}$$

$$T_2^{(1)}(q^2) = \frac{2\sqrt{E_V M_B}}{M_B^2 - M_V^2}\int\frac{d^3p}{(2\pi)^3}\bar\Psi_V\left(\mathbf{p} + \frac{2\epsilon_q}{E_V+M_V}\boldsymbol\Delta\right)\sqrt{\frac{\epsilon_f(p+\Delta)+m_f}{2\epsilon_f(p+\Delta)}}\sqrt{\frac{\epsilon_b(p)+m_b}{2\epsilon_b(p)}}$$

$$\times\left\{(M_B - E_V)\left[1 + \frac{\mathbf{p}^2/3 + (\mathbf{p}\boldsymbol\Delta)}{(\epsilon_f(p+\Delta)+m_f)(\epsilon_b(p)+m_b)} +\right.\right.$$

$$\left.\frac{\mathbf{p}^2\boldsymbol\Delta^2}{3(E_V+M_V)(\epsilon_q(p)+m_q)(\epsilon_f(p+\Delta)+m_f)(\epsilon_b(p)+m_b)}\right]$$

$$+\boldsymbol\Delta^2\left[\frac{1}{\epsilon_f(p+\Delta)+m_f} + \frac{(\mathbf{p}\boldsymbol\Delta)}{\boldsymbol\Delta^2}\left(\frac{1}{\epsilon_f(p+\Delta)+m_f} + \frac{1}{\epsilon_b(p)+m_b}\right)\right.$$

$$-\frac{\mathbf{p}^2}{3(E_V+M_V)}\left(\frac{1}{\epsilon_q(p)+m_q}\left(\frac{1}{\epsilon_b(p)+m_b} - \frac{1}{\epsilon_f(p+\Delta)+m_f}\right)\right.$$

$$\left.\left.\left.\left.+\frac{2}{(\epsilon_f(p)+m_f)^2}\right)\right]\right]\right\}\Psi_B(\mathbf{p}), \tag{A.10}$$

$$T_2^{S(2)}(q^2) = \frac{2\sqrt{E_V M_B}}{M_B^2 - M_V^2}\int\frac{d^3p}{(2\pi)^3}\bar\Psi_V\left(\mathbf{p} + \frac{2\epsilon_q}{E_V+M_V}\boldsymbol\Delta\right)\sqrt{\frac{\epsilon_f(p+\Delta)+m_f}{2\epsilon_f(p+\Delta)}}$$

$$\times\left\{\frac{\epsilon_f(p+\Delta)-m_f}{2\epsilon_f(p+\Delta)(\epsilon_f(p+\Delta)+m_f)}\left(M_B - E_V + \frac{(\mathbf{p}\boldsymbol\Delta)}{2m_b}\right)\right.$$

$$\times\left(M_V - \epsilon_f\left(p + \frac{2\epsilon_q}{E_V+M_V}\Delta\right) - \epsilon_q\left(p + \frac{2\epsilon_q}{E_V+M_V}\Delta\right)\right)$$

$$-(\mathbf{p}\boldsymbol\Delta)\left(\frac{M_B + M_V - \epsilon_b(p) - \epsilon_q(p) - \epsilon_f\left(p + \frac{2\epsilon_q}{E_V+M_V}\Delta\right) - \epsilon_q\left(p + \frac{2\epsilon_q}{E_V+M_V}\Delta\right)}{2m_b(\epsilon_b(p+\Delta)+m_b)}\right.$$

$$\left.\left.+\frac{M_B - M_V - \epsilon_b(p) - \epsilon_q(p) + \epsilon_f\left(p + \frac{2\epsilon_q}{E_V+M_V}\Delta\right) + \epsilon_q\left(p + \frac{2\epsilon_q}{E_V+M_V}\Delta\right)}{2\epsilon_f(p+\Delta)(\epsilon_f(p+\Delta)+m_f)}\right)\right\}\Psi_B(\mathbf{p}),$$
$$\tag{A.11}$$

$$T_2^{V(2)}(q^2) = \frac{2\sqrt{E_V M_B}}{M_B^2 - M_V^2}\int\frac{d^3p}{(2\pi)^3}\bar\Psi_V\left(\mathbf{p} + \frac{2\epsilon_q}{E_V+M_V}\boldsymbol\Delta\right)\sqrt{\frac{\epsilon_f(p+\Delta)+m_f}{2\epsilon_f(p+\Delta)}}$$

$$\times\left\{\frac{\epsilon_f(p+\Delta)-m_f}{2\epsilon_f(p+\Delta)(\epsilon_f(p+\Delta)+m_f)}\left(M_B - E_V + \frac{(\mathbf{p}\boldsymbol\Delta)}{2m_b}\right)\right.$$

$$\times\left(M_V - \epsilon_f\left(p + \frac{2\epsilon_q}{E_V+M_V}\Delta\right) - \epsilon_q\left(p + \frac{2\epsilon_q}{E_V+M_V}\Delta\right)\right)$$

$$+(\mathbf{p}\boldsymbol{\Delta})\left(\frac{M_V - \epsilon_f\left(p + \frac{2\epsilon_q}{E_V + M_V}\Delta\right) - \epsilon_q\left(p + \frac{2\epsilon_q}{E_V + M_V}\Delta\right)}{2m_b(\epsilon_b(p+\Delta) + m_b)}\right.$$

$$\left.\left.+\frac{M_B - \epsilon_b(p) - \epsilon_q(p)}{2\epsilon_f(p+\Delta)(\epsilon_f(p+\Delta) + m_f)}\right)\right\}\Psi_B(\mathbf{p}), \tag{A.12}$$

$$T_3(q^2) = T_3^{(1)}(q^2) + \varepsilon T_3^{S(2)}(q^2) + (1-\varepsilon)T_3^{V(2)}(q^2), \tag{A.13}$$

$$T_3^{(1)}(q^2) = \sqrt{\frac{E_V}{M_B}} \int \frac{d^3p}{(2\pi)^3} \bar{\Psi}_V\left(\mathbf{p} + \frac{2\epsilon_q}{E_V + M_V}\boldsymbol{\Delta}\right)\sqrt{\frac{\epsilon_f(p+\Delta) + m_f}{2\epsilon_f(p+\Delta)}}\sqrt{\frac{\epsilon_b(p) + m_b}{2\epsilon_b(p)}}$$

$$\times\left\{-\left(1 + \frac{\mathbf{p}^2/3 - (\mathbf{p}\boldsymbol{\Delta})}{(\epsilon_f(p+\Delta) + m_f)(\epsilon_b(p) + m_b)} + \right.\right.$$

$$\left.\frac{2\mathbf{p}^2\boldsymbol{\Delta}^2}{3(E_V + M_V)(\epsilon_f(p+\Delta) + m_f)^2(\epsilon_b(p) + m_b)}\right) + \frac{M_B E_V + M_V^2}{M_B}\left[\frac{1}{\epsilon_f(p+\Delta) + m_f}\right.$$

$$+\frac{(\mathbf{p}\boldsymbol{\Delta})}{\boldsymbol{\Delta}^2}\left(\frac{1}{\epsilon_f(p+\Delta) + m_f} + \frac{1}{\epsilon_b(p) + m_b} + \frac{2(M_B - E_V)}{(\epsilon_f(p+\Delta) + m_f)(\epsilon_b(p) + m_b)}\right)$$

$$-\frac{\mathbf{p}^2}{3(E_V + M_V)}\left(\frac{1}{\epsilon_q(p) + m_q}\left(\frac{1}{\epsilon_b(p) + m_b} - \frac{1}{\epsilon_f(p+\Delta) + m_f}\right)\right.$$

$$+\frac{2}{(\epsilon_f(p) + m_f)^2} + \frac{M_B - E_V}{(\epsilon_f(p+\Delta) + m_f)(\epsilon_b(p) + m_b)}$$

$$\left.\left.\left.\times\left(\frac{2}{\epsilon_f(p+\Delta) + m_f} - \frac{1}{\epsilon_q(p) + m_q}\right)\right)\right]\right\}\Psi_B(\mathbf{p}), \tag{A.14}$$

$$T_3^{S(2)}(q^2) = \sqrt{\frac{E_V}{M_B}} \int \frac{d^3p}{(2\pi)^3} \bar{\Psi}_V\left(\mathbf{p} + \frac{2\epsilon_q}{E_V + M_V}\boldsymbol{\Delta}\right)\sqrt{\frac{\epsilon_f(p+\Delta) + m_f}{2\epsilon_f(p+\Delta)}}$$

$$\times\left\{\frac{\epsilon_f(p+\Delta) - m_f}{2\epsilon_f(p+\Delta)(\epsilon_f(p+\Delta) + m_f)}\left(\frac{M_B E_V + M_V^2}{2M_B m_b}\frac{(\mathbf{p}\boldsymbol{\Delta})}{\boldsymbol{\Delta}^2} - 1\right)\right.$$

$$\times\left(M_V - \epsilon_f\left(p + \frac{2\epsilon_q}{E_V + M_V}\Delta\right) - \epsilon_q\left(p + \frac{2\epsilon_q}{E_V + M_V}\Delta\right)\right) - \frac{M_B E_V + M_V^2}{M_B}\frac{(\mathbf{p}\boldsymbol{\Delta})}{\boldsymbol{\Delta}^2}$$

$$\times\left(\frac{M_B + M_V - \epsilon_b(p) - \epsilon_q(p) - \epsilon_f\left(p + \frac{2\epsilon_q}{E_V + M_V}\Delta\right) - \epsilon_q\left(p + \frac{2\epsilon_q}{E_V + M_V}\Delta\right)}{2m_b(\epsilon_b(p+\Delta) + m_b)}\right.$$

$$\left.\left.+\frac{M_B - M_V - \epsilon_b(p) - \epsilon_q(p) + \epsilon_f\left(p + \frac{2\epsilon_q}{E_V + M_V}\Delta\right) + \epsilon_q\left(p + \frac{2\epsilon_q}{E_V + M_V}\Delta\right)}{2\epsilon_f(p+\Delta)(\epsilon_f(p+\Delta) + m_f)}\right)\right\}\Psi_B(\mathbf{p}),$$

$$\tag{A.15}$$

$$T_3^{V(2)}(q^2) = \sqrt{\frac{E_V}{M_V}} \int \frac{d^3p}{(2\pi)^3} \bar{\Psi}_V\left(\mathbf{p} + \frac{2\epsilon_q}{E_V + M_V}\boldsymbol{\Delta}\right)\sqrt{\frac{\epsilon_f(p+\Delta) + m_f}{2\epsilon_f(p+\Delta)}}$$

$$\times\left\{\frac{\epsilon_f(p+\Delta) - m_f}{2\epsilon_f(p+\Delta)(\epsilon_f(p+\Delta) + m_f)}\left(\frac{M_B E_V + M_V^2}{2M_B m_b}\frac{(\mathbf{p}\boldsymbol{\Delta})}{\boldsymbol{\Delta}^2} - 1\right)\right.$$

$$\times \left(M_V - \epsilon_f \left(p + \frac{2\epsilon_q}{E_V + M_V}\Delta \right) - \epsilon_q \left(p + \frac{2\epsilon_q}{E_V + M_V}\Delta \right) \right)$$
$$+ \frac{M_B E_V + M_V^2}{M_B} \frac{(\mathbf{p}\boldsymbol{\Delta})}{\boldsymbol{\Delta}^2} \left(\frac{M_V - \epsilon_f \left(p + \frac{2\epsilon_q}{E_V + M_V}\Delta \right) - \epsilon_q \left(p + \frac{2\epsilon_q}{E_V + M_V}\Delta \right)}{2m_b(\epsilon_b(p + \Delta) + m_b)} \right.$$
$$\left. \left. + \frac{M_B - \epsilon_b(p) - \epsilon_q(p)}{2\epsilon_f(p + \Delta)(\epsilon_f(p + \Delta) + m_f)} \right) \right\} \Psi_B(\mathbf{p}), \tag{A.16}$$

where $V = K^*, D_s^*, D^*$ and

$$\Delta \equiv |\boldsymbol{\Delta}| = \sqrt{\frac{(M_B^2 + M_V^2 - q^2)^2}{4M_B^2} - M_V^2}, \qquad E_V = \sqrt{M_V^2 + \boldsymbol{\Delta}^2}.$$

[1] U. Egede, T. Hurth, J. Matias, M. Ramon and W. Reece, arXiv:1005.0571 [hep-ph]; JHEP **11**, 032 (2008).

[2] W. Altmannshofer, A. J. Buras, D. M. Straub and M. Wick, JHEP **04**, 022 (2009).

[3] For recent review see, e.g., T. Hurth and M. Nakao, arXiv:1005.1224 [hep-ph] and references therein.

[4] J. Charles, A. Le Yaouanc, L. Oliver, O. Pene and J. C. Raynal, Phys. Rev. D **60**, 014001 (1999).

[5] C. W. Bauer, S. Fleming, D. Pirjol and I. W. Stewart, Phys. Rev. D **63**, 114020 (2001); C. W. Bauer, D. Pirjol and I. W. Stewart, Phys. Rev. D **65**, 054022 (2002); M. Beneke, A. P. Chapovsky, M. Diehl and T. Feldmann, Nucl. Phys. B **643**, 431 (2002); R. J. Hill and M. Neubert, Nucl. Phys. B **657**, 229 (2003).

[6] B. Aubert *et al.* [BABAR Collaboration], Phys. Rev. D **73**, 092001 (2006).

[7] J. T. Wei *et al.* [BELLE Collaboration], Phys. Rev. Lett. **103**, 171801 (2009).

[8] T. Aaltonen *et al.* [CDF Collaboration], Phys. Rev. D **79**, 011104 (2009).

[9] CDF Collaboration, CDF note 10047.

[10] M. Artuso *et al.*, Eur. Phys. J. C **57**, 309 (2008); The LHCb Collaboration, arXiv:0912.4179.

[11] A. Faessler, T. Gutsche, M. A. Ivanov, J. G. Körner and V. E. Lyubovitskij, Eur. Phys. J. direct C **4**, 18 (2002).

[12] C. Q. Geng, C. W. Hwang and C. C. Liu, Phys. Rev. D **65**, 094037 (2002).

[13] H. M. Choi, Phys. Rev. D **81**, 054003 (2010).

[14] K. Azizi, F. Falahati, V. Bashiry and S. M. Zebarjad, Phys. Rev. D **77**, 114024 (2008); K. Azizi and R. Khosravi, Phys. Rev. D **78**, 036005 (2008).

[15] D. Ebert, R. N. Faustov and V. O. Galkin, Phys. Rev. D **75**, 074008 (2007).

[16] D. Ebert, R. N. Faustov and V. O. Galkin, Phys. Rev. D **68**, 094020 (2003).

[17] D. Ebert, R. N. Faustov and V. O. Galkin, Eur. Phys. J. C **32**, 29 (2003).

[18] R. N. Faustov and V. O. Galkin, Phys. Rev. D **52**, 5131 (1995); D. Ebert, R. N. Faustov, V. O. Galkin and H. Toki, Phys. Rev. D **64**, 054001 (2001).

[19] D. Ebert, R. N. Faustov and V. O. Galkin, Phys. Rev. D **67**, 014027 (2003).

[20] D. Ebert, V. O. Galkin and R. N. Faustov, Phys. Rev. D **57**, 5663 (1998) [Erratum-ibid. D **59**, 019902 (1999)]; D. Ebert, R. N. Faustov and V. O. Galkin, Eur. Phys. J. C **66**, 197 (2010).

[21] R. N. Faustov and V. O. Galkin, Z. Phys. C **66**, 119 (1995).

[22] D. Ebert, R. N. Faustov and V. O. Galkin, Phys. Rev. D **64**, 094022 (2001).

[23] G. Buchalla, G. Hiller and G. Isidori, Phys. Rev. D **63**, 014015 (2000).

[24] G. Buchalla, A. J. Buras and M. E. Lautenbacher, Rev. Mod. Phys. **68**, 1125 (1996).

[25] A. Ali, P. Ball, L. T. Handoko and G. Hiller, Phys. Rev. D **61**, 074024 (2000).

[26] D. Melikhov, N. Nikitin and S. Simula, Phys. Rev. D **57**, 6814 (1998).

[27] A. J. Buras and M. Munz, Phys. Rev. D **52**, 186 (1995).

[28] D. Ebert, R. N. Faustov and V. O. Galkin, Phys. Rev. D **73**, 094002 (2006).

[29] R. N. Faustov, Ann. Phys. **78**, 176 (1973); Nuovo Cimento A **69**, 37 (1970).

[30] C. Amsler *et al.* (Particle Data Group), Phys. Lett. B667, 1 (2008).

[31] D. Melikhov and B. Stech, Phys. Rev. D **62**, 014006 (2000).

[32] M. Misiak and J. Urban, Phys. Lett. B **451**, 161 (1999).

[33] B. Aubert *et al.* [BABAR Collaboration], Phys. Rev. D **78**, 072007 (2008).

[34] K. F. Chen *et al.* [BELLE Collaboration], Phys. Rev. Lett. **99**, 221802 (2007).

[35] E. Barberio *et al.* [Heavy Flavor Averaging Group], arXiv:0808.1297 [hep-ex].